National Institute of Chemistry
Slovenia

Characterization of Complex Macromolecular and Supramolecular Structures by AF4 / SEC – MALS(DLS)

Ema Žagar
ema.zagar@ki.si

National Institute of Chemistry
Department of Polymer Chemistry and Technology
Hajdrihova 19, 1000 Ljubljana, Slovenia

Polymer Characterization Summit, Dernbach, September 20th – 21st, 2018

Asymmetric-Flow Field-Flow Fractionation (AF4)

ADVANTAGES

- Large separation range: nm - µm.
- Great separation power in sub-micrometer range.
- No degradation due to shear forces.
- Separation of MM in solution and particles in emulsions / suspensions.
- Flexible separation of inhomogenous samples.
- Fractions can be collected and used for off-line analysis.
- Medium: aqueous or organic.

LIMITATIONS

- **Lower size limit** is determined by membrane cut off and maximum flow through the membrane.
- **Upper size limit** is set by inversion of elution order by steric elution - depends on particle shape and size (600 nm - 2000 nm).

AF4(SEC) coupled to MALS(QELS)-UV-RI detectors

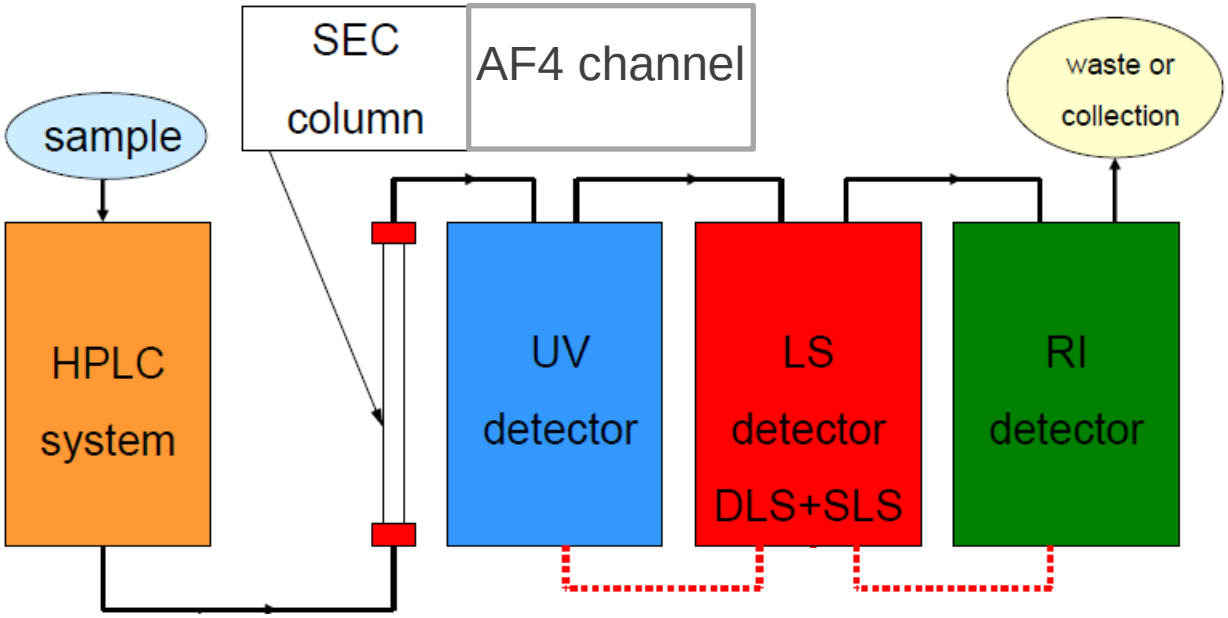

- Absolute MMA: M_n, M_w
- Molar-mass distribution described by the dispersity, $Đ_M = M_w/M_n$
- Radius of gyration: R_g
- Hydrodynamic radius: R_h
- MM conformation, particle shape: R_g/R_h or log(R_g) vs. log(M)
- Chemical composition along the molar mass distribution of complex two component systems, e.g., **copolymers, protein conjugates, glycosylated proteins, membrane protein/detergent complexes**, if the response factors of UV and RI detectors for these two components are sufficiently different.

SLS

Radius of gyration or RMS - R_g

$$R_g^2 = \frac{\sum m_i r_i^2}{\sum m_i}$$

R_g or RMS – average (root mean square) distance of each mass point in a molecule from the molecule's center of gravity.

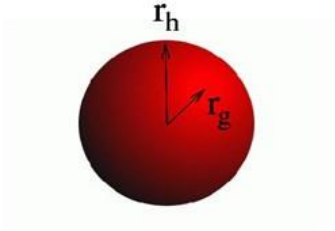

$$\rho = \frac{r_g}{r_h} = 0.77$$

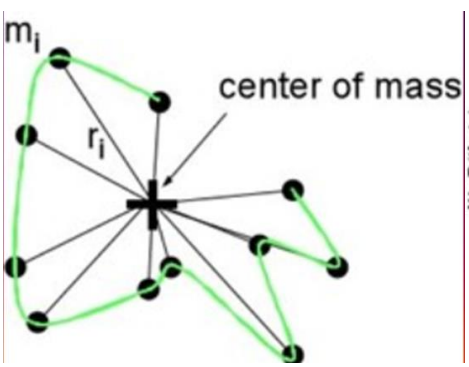

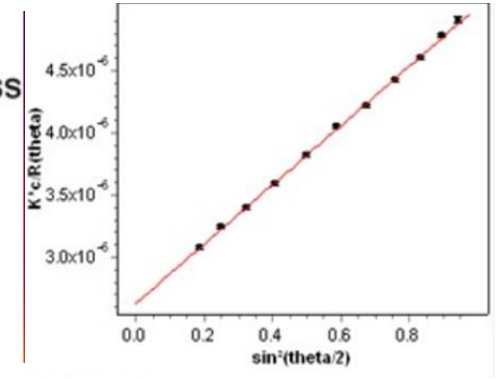

DLS

Hydrodynamic radius - R_h

Stokes-Einstein equation:

$$R_h = \frac{k_B T}{6\pi\eta D}$$

R_h – radius of a hard sphere with the same diffusion coefficient as the particle under examination.

Scattered light intensity is measured through time

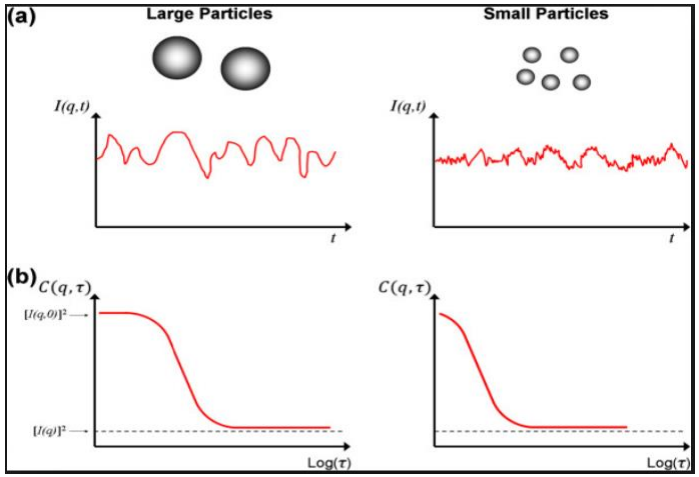

Theory of MALS-UV-RI Detection

For the copolymers – an example is given for PS_yPI_x copolymers (the same is valid for membrane protein-detergent complex, pegylated/glycosolated proteins), etc.

$$\left(\frac{dn}{dc}\right)_{PS_yPI_x} = \left(\frac{dn}{dc}\right)_{PS} \cdot wt_{PS} + \left(\frac{dn}{dc}\right)_{PI} \cdot wt_{PI} = \left(\frac{dn}{dc}\right)_{PS} \cdot wt_{PS} + \left(\frac{dn}{dc}\right)_{PI} \cdot (1 - wt_{PS})$$

$$\varepsilon_{PS_yPI_x} = \varepsilon_{PS} \cdot wt_{PS} + \varepsilon_{PI} \cdot (1 - wt_{PS}) \Rightarrow \varepsilon_{PS_yPI_x} = \varepsilon_{PS} \cdot wt_{PS}$$

$$c_{RI}(PS_yPI_x) = \frac{I_{RI}}{K_{RI} \cdot \left(\frac{dn}{dc}\right)_{PS_yPI_x}} \equiv c_{UV}(PS_yPI_x) = \frac{I_{UV}}{K_{UV} \cdot \varepsilon_{PS_yPI_x}} = \frac{I_{UV}}{K_{UV} \cdot \varepsilon_{PS} \cdot wt_{PS}} \Rightarrow$$

$$\frac{I_{RI}}{K_{RI}\left[\left(\frac{dn}{dc}\right)_{PS} \cdot wt_{PS} + \left(\frac{dn}{dc}\right)_{PI} \cdot (1 - wt_{PS})\right]} = \frac{I_{UV}}{K_{UV} \cdot (\varepsilon_{PS} \cdot wt_{PS})} \Rightarrow wt_{PS}$$

$$M(PS_yPI_x) \propto \frac{I_{LS}}{\left(\frac{dn}{dc}\right)^2_{PS_yPI_x} \cdot c_{PS_yPI_x}}$$

$$M_{PS_y} = \frac{K_{RI}^2}{K_{LS}K_{UV}} \frac{I_{LS}I_{UV}}{\varepsilon_{PS}I_{RI}^2}$$

AF4/MALS-DLS of lipid vesicles, lipid droplets and PS latex particles

Large unilamellar Vesicles - LUV

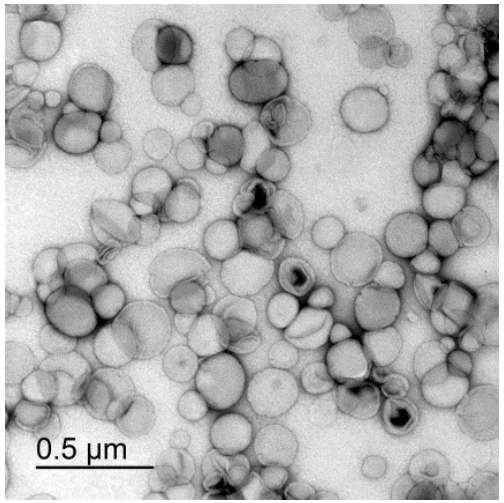

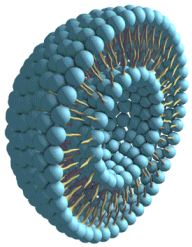

Broad size distribution
R_h: 80 and 200 nm
Composition: SM/Chol
1:1 (LUV11); 4:1 (LUV41)

Lipid droplets - LD

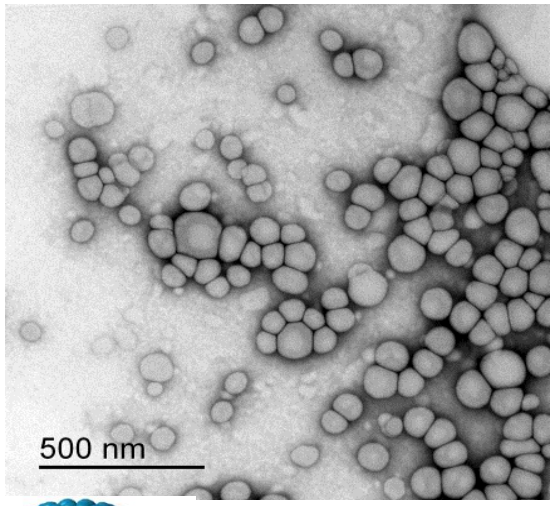

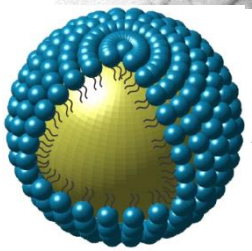

Broad size distribution
R_h: 55 nm
Composition: SM/Chol/TOG
1/1/5 (LD11); 4/1/12 (LD41)

PS latex particles

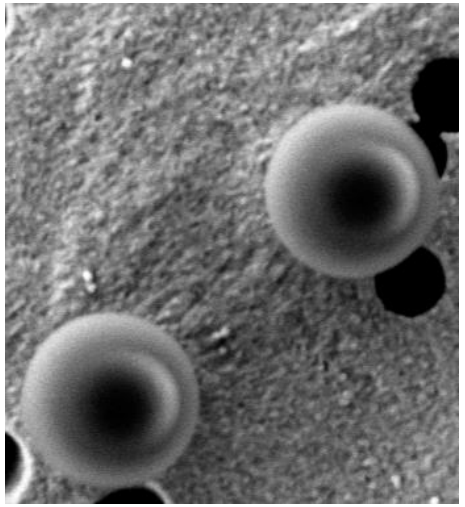

Narrow size distribution
R_h: 30, 50, 100, 250 nm

Goal:

i) Monitoring LUV size and shape by MALS in dependence of the detector flow rate conditions (0.2, 0.5, and 1 mL/min) to perceive possible changes in vesicle shape as a consequence of particle deformation in flow;

ii) to estimate a range of detector flow velocities (passage flow at the detector) at which the particle sizing by flow-DLS is still accurate.

J. Chromatography A **2015**, *1418,* 185−193
Anal. Chem. ***2017****, 89,* 11744−11752

LUV and LD of different size and composition

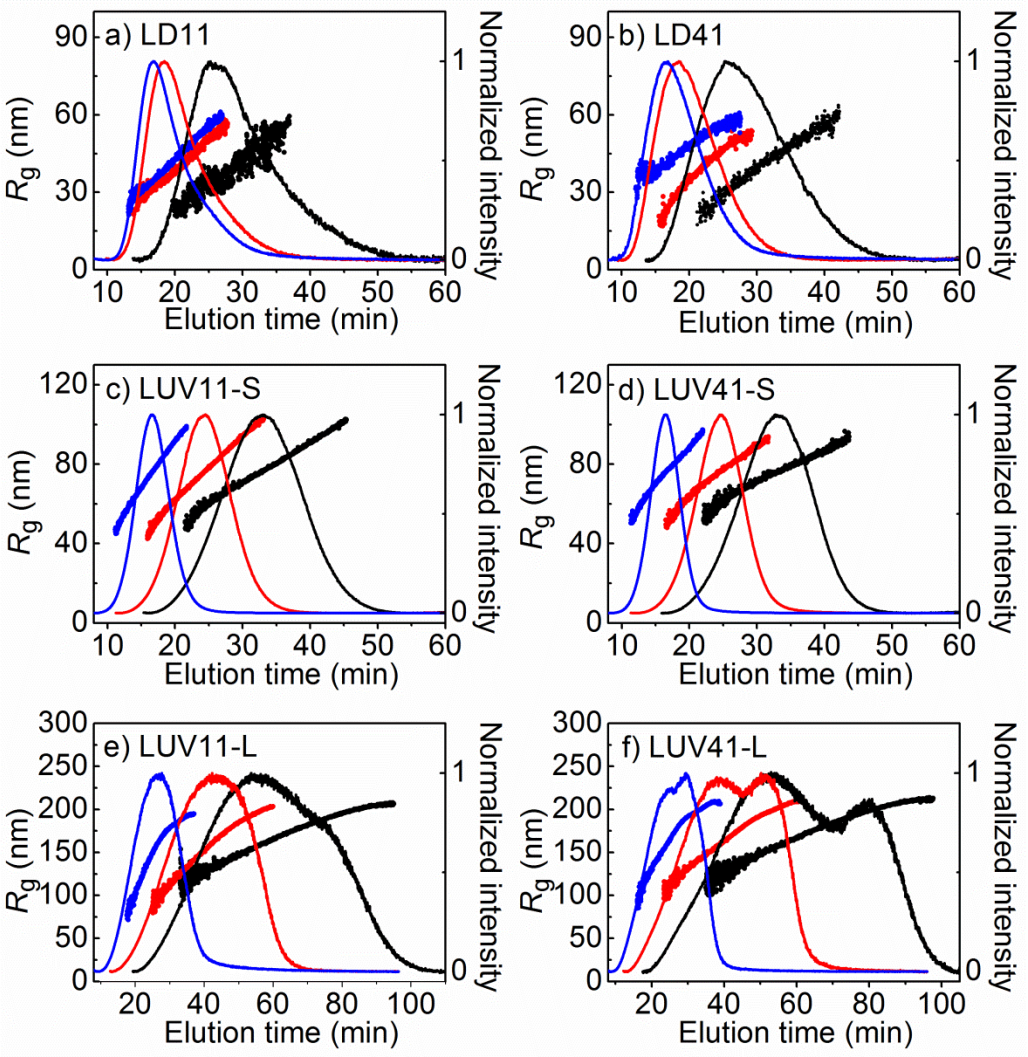

Experimental conditions:

- Trapezoidal-shaped channel: 350 µm spacer and RC membrane (10 kDa cut-off).
- Mobile phase: 10 mM Hepes buffer; pH = 8.0.
- Injection: in focus mode at 0.2 mL/min over 3 min, and additional focusing of 2 min.
- 30, 50, and 100 nm PS standards and LD: at 0.2, 0.5, and 1 mL/min detector flow rates the cross-flow gradients were from 0.2 to 0.09 in 80 min, from 0.3 to 0.09 in 80 min, and from 0.5 to 0.09 in 80 min, respectively.
- 250 nm PS standards and LUV: Cross-flow gradients were from 0.2 to 0.09 in 90 min at 0.5 and 1 mL/min detector flow rates. At 0.2 mL/min detector flow rate a constant cross-flow of 0.1 mL/min for 90 min was used.

AF4-MALS fractograms (solid curves: normalized LS intensities at 90° angle) together with R_g from MALS for LD and LUV of different composition and size obtained at different laminar flow rates: **0.2 mL/min**; **0.5 mL/min**; and **1 mL/min**.

LUV and LD of different size and composition

R_h and R_g determined by DLS and MALS, respectively, in batch and flow mode at various detector flow velocities for LUV and LD samples.

	R_h (flow) [nm]			R_h (batch) [nm]	R_g (flow) [nm]			R_g (batch) [nm]
detector flow [mL/min]	0.2	0.5	1.0		0.2	0.5	1.0	
Sample								
LD11	55	47	40	56	45	43	42	44
LD41	55	48	44	57	43	43	43	44
LUV11-S	76	61	41	75	80	80	80	77
LUV41-S	79	61	41	78	77	77	77	75
LUV11-L	189	136	85	192	186	183	185	186
LUV41-L	198	129	81	195	190	191	190	191

PS latex particles - nanosphere size standards

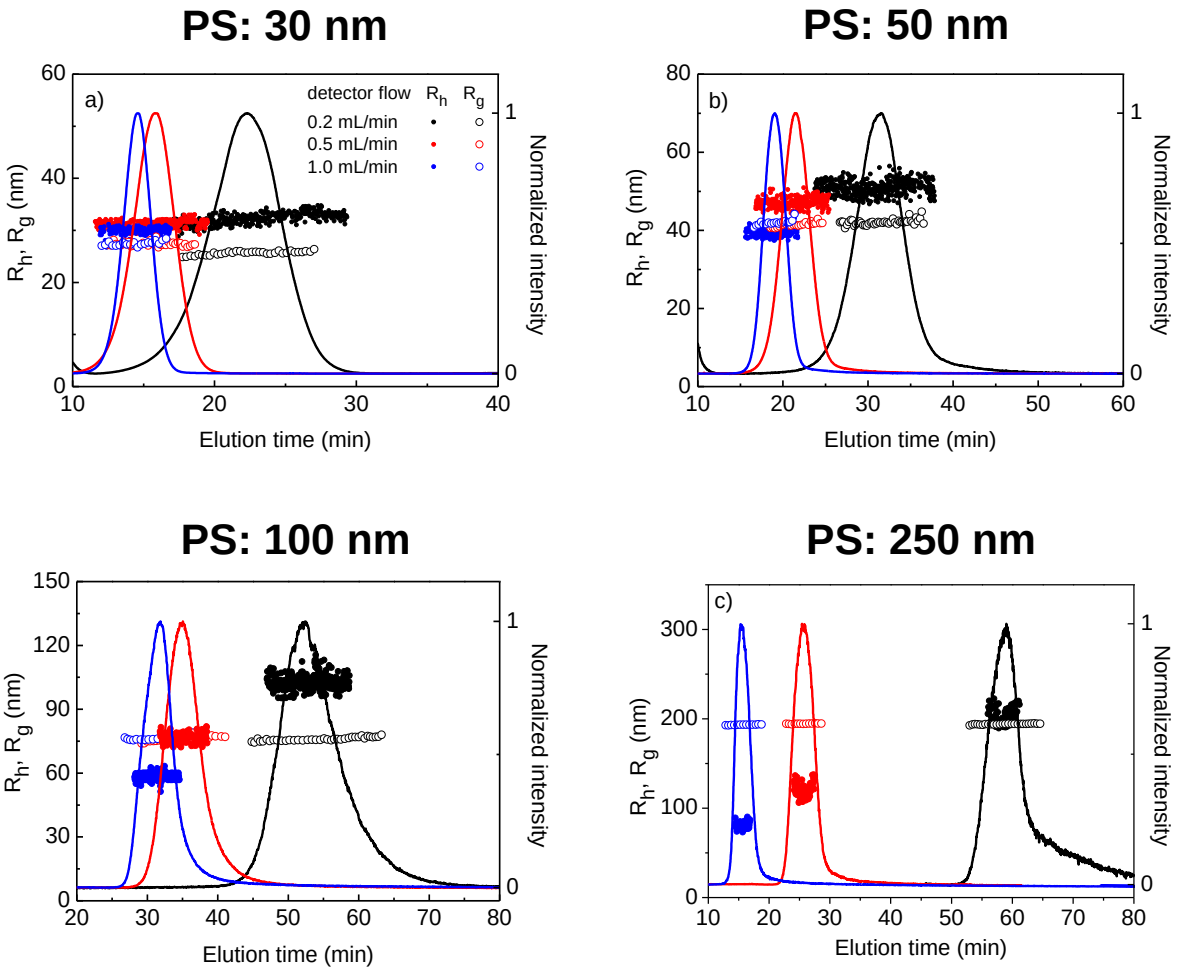

AF4-MALS fractograms together with R_h (● ● ●) and R_g (**ooo**) at detector flow rate of **0.2 mL/min**; **0.5 mL/min**; **1 mL/min**.

PS nanosphere size standards

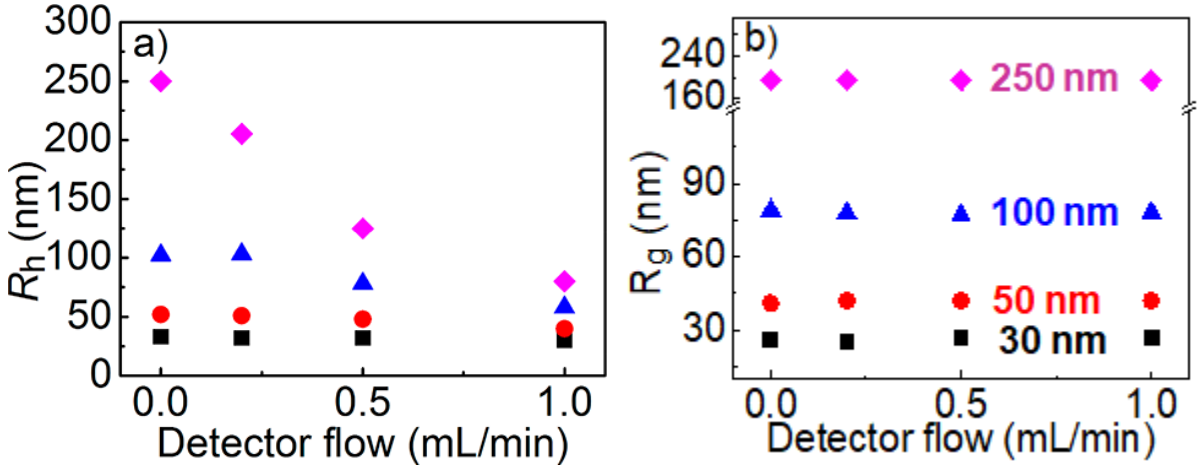

LUV and LD

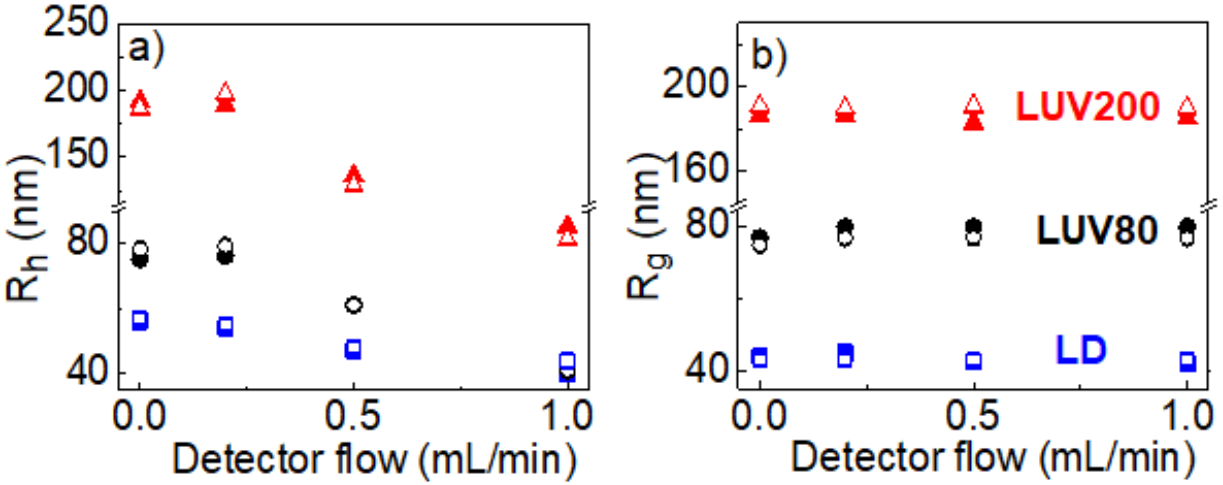

R_h and R_g as a function of detector flow rate. Values at detector flow rate of 0 mL/min correspond to batch DLS and SLS.

LUV and LD of different size and composition

Shape factor:

Spherical shell structure (LUV)
$R_g/R_h \sim 1.0$

Homogenous sphere (LD, PS)
$R_g/R_h \sim 0.775$

Shape factor calculated from batch SLS and DLS and from AF4/MALS-DLS for all LUV and LD samples.

Sample	R_g/R_h Batch mode	R_g/R_h AF4 (0.2 mL/min)
LD11	0.79	0.82
LD41	0.77	0.78
LUV11-S	1.03	1.05
LUV41-S	0.96	0.97
LUV11-L	0.97	0.98
LUV41-L	0.98	0.96

Monodispersed 100 nm PS nanosphere standard

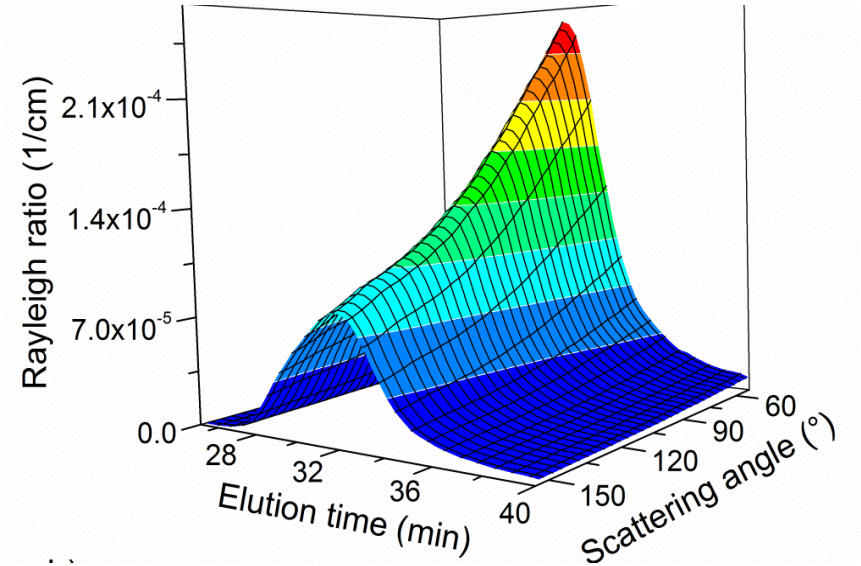

Polydispersed 80 nm LUV

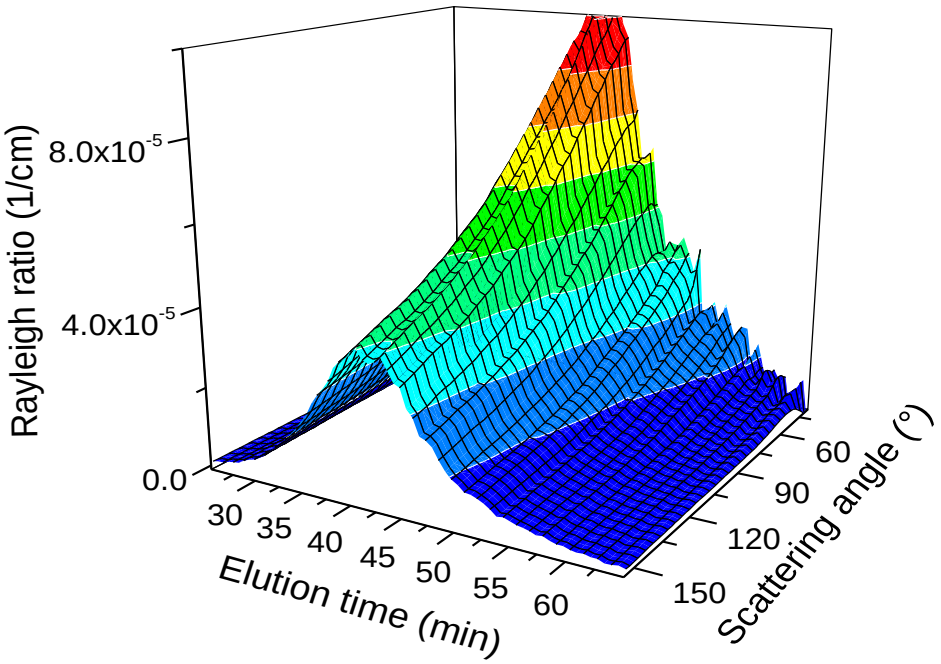

3D plot: angular dependences of scattered light as a function of elution time for 100 nm PS nanosphere size standard (left) and small 80 nm LUV (right).

Monodispersed 250 nm PS nanosphere standard

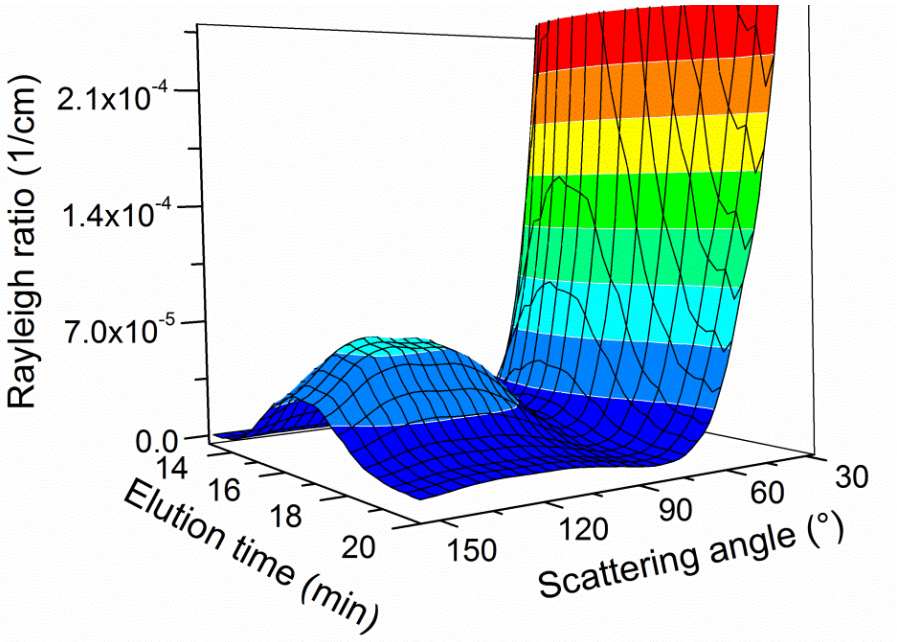

Polydispersed 200 nm LUV

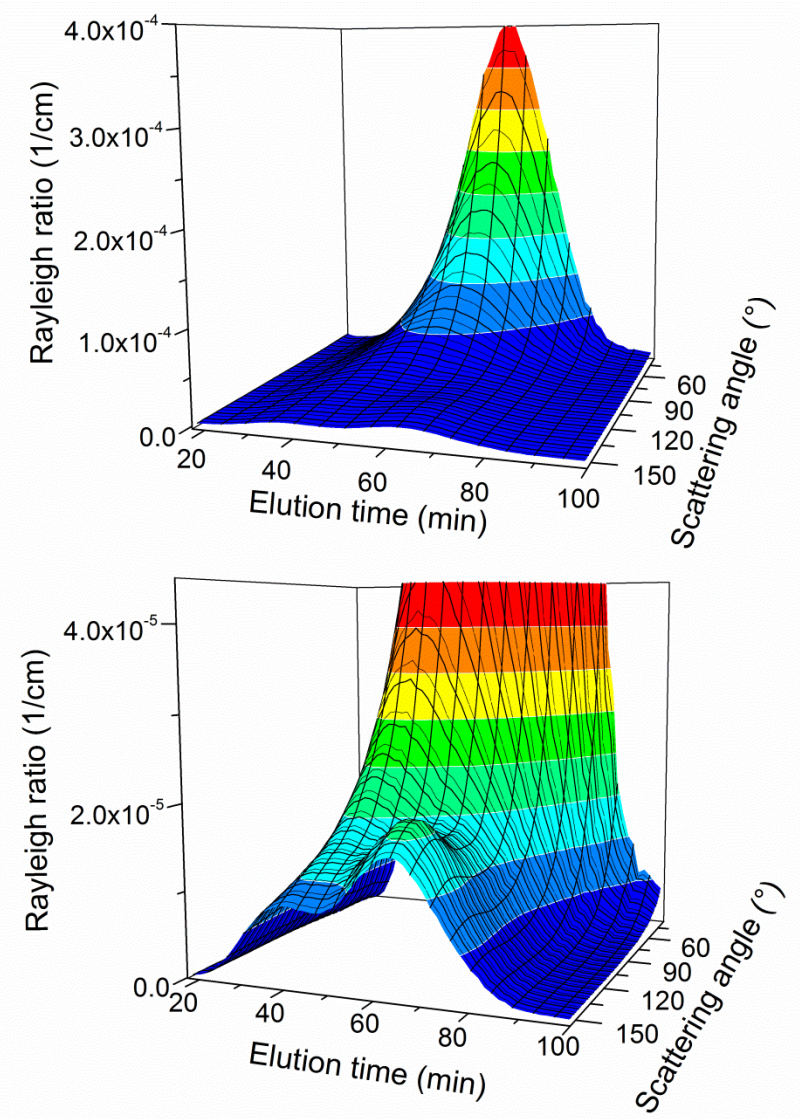

3D plot: angular dependences of scattered light as a function of elution time for 250 nm PS nanosphere size standard (left) and large 200 nm LUV (right). The bottom figure shows enlargement at larger angles.

Angular dissymmetry factor at 43° angle

Detector flow rate: 0.2 mL/min **1 mL/min**

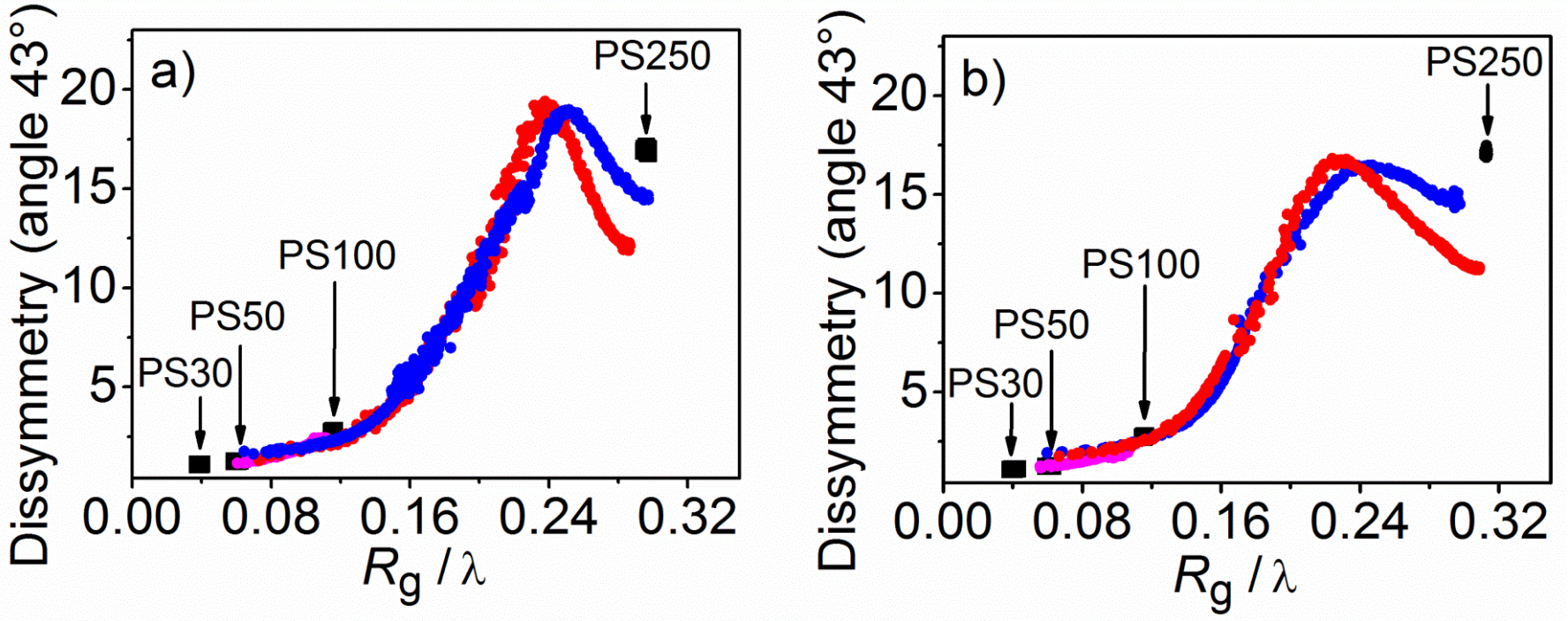

Dissymmetry factors calculated at a 43° angle for PS standards with radii of 30, 50, 100, and 250 nm, as well as for **LUV11-S (magenta)**, **LUV11-L (blue)**, and **LUV41-L (red)** at a detector flow rate of (a) 0.2 mL/min and (b) 1 mL/min.

AF4-MALS fractograms

Kratky plots

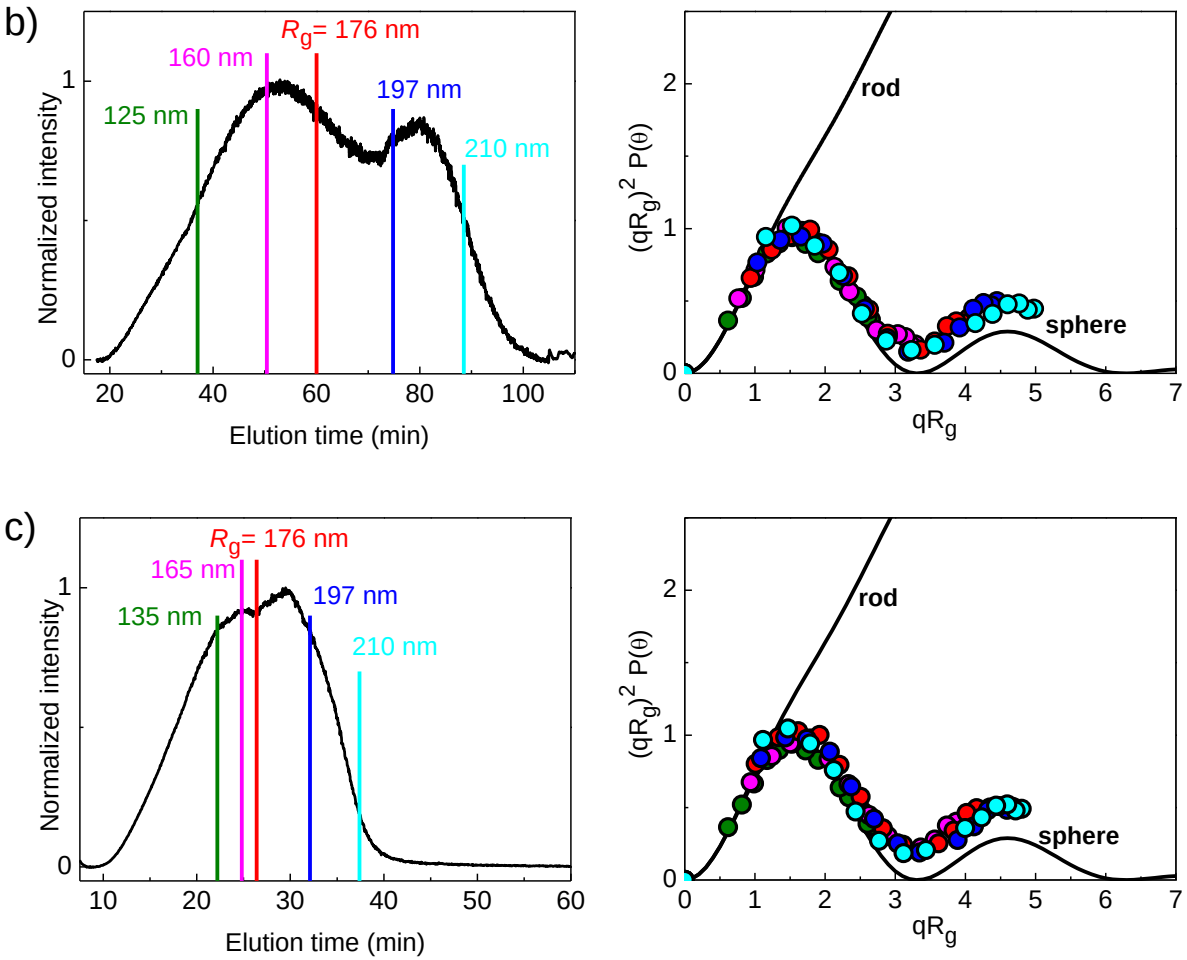

Detector flow rate: 0.2 mL/min

Detector flow rate: 1 mL/min

Colored symbols represent Kratky plots of LUV11-L fractions eluted at different elution times as depicted with the colored dashed lines in the fractograms; detector flow rates: 0.2 and 1 mL/min.

Exosomes - Size characterization and Quantification by AF4/MALS

Exosomes:
R_{rms} = 113 nm
R_{geom} = 127 nm
R_{rms}/ R_h = 0.84
Number density:
1.1 x 10^{10} particles/mL

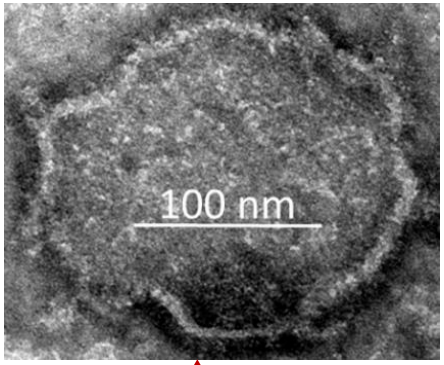

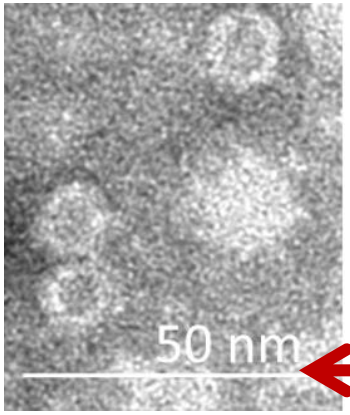

Small vesicles +
protein impurities
R_{rms} = 23 nm
R_{geom} = 24 nm

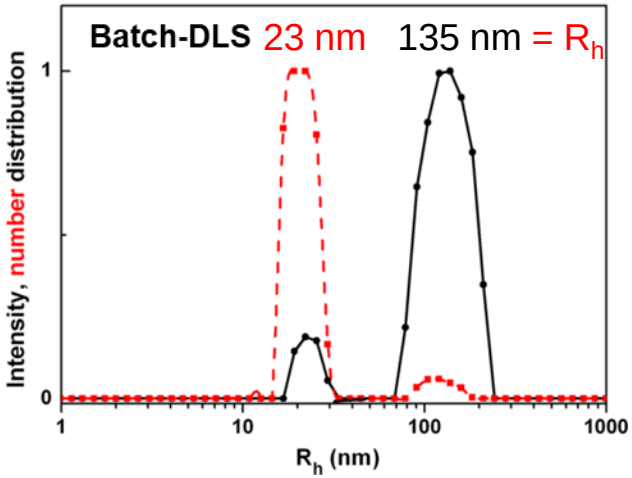

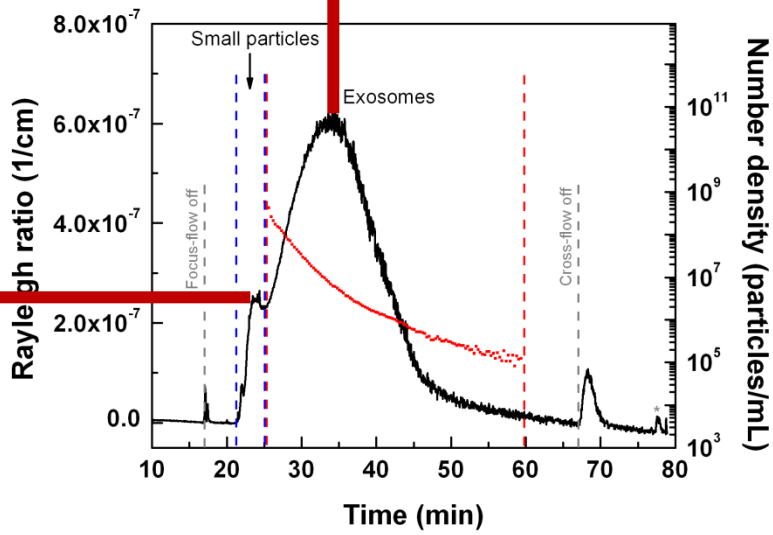

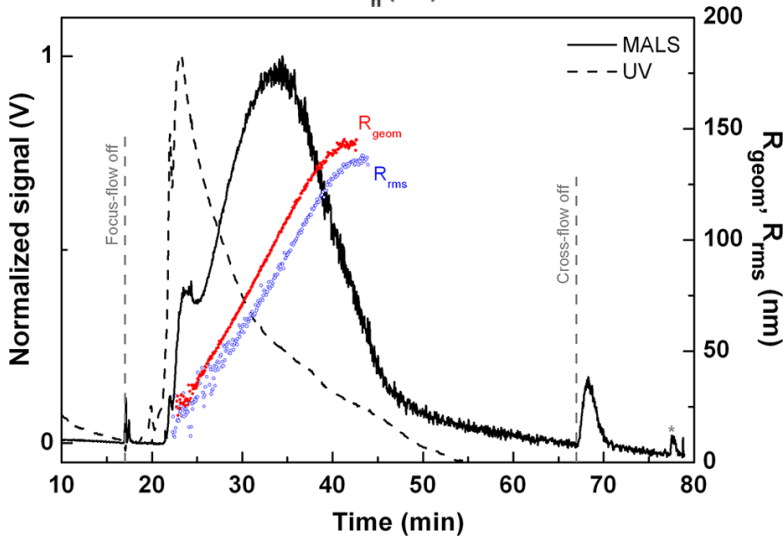

AF4 fractogram of exosome sample in PBS buffer, pH = 7.4 together with number density, geometric radius (R_{geom}), and root-mean-square radius (R_{rms}) distributions.
Cross-flow conditions: 3 - 0.25 mL/min in 5 min and 0.25 - 0.09 in 45 min.

Anal. Chem. **2015**, *87,* 9225−9233

Poly(Styrene-*b*-Isoprene) Miktoarm Star Copolymers $PS(PI)_x$; x = 2, 3, 5, and 7

Synthesis: anionic polymerization of homopolymers and subsequent coupling of PSLi and PILi homopolimers to multifunctional chlorosilane linking agents.

$PS(PI)_2$ CH_3SiCl_3

$PS(PI)_3$ $SiCl_4$

$PS(PI)_5$ $Cl_3SiCH_2CH_2SiCl_3$

$PS(PI)_7$

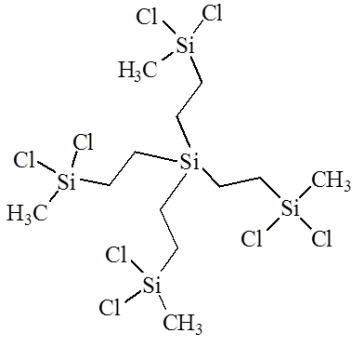

8 functional chlorosilane core

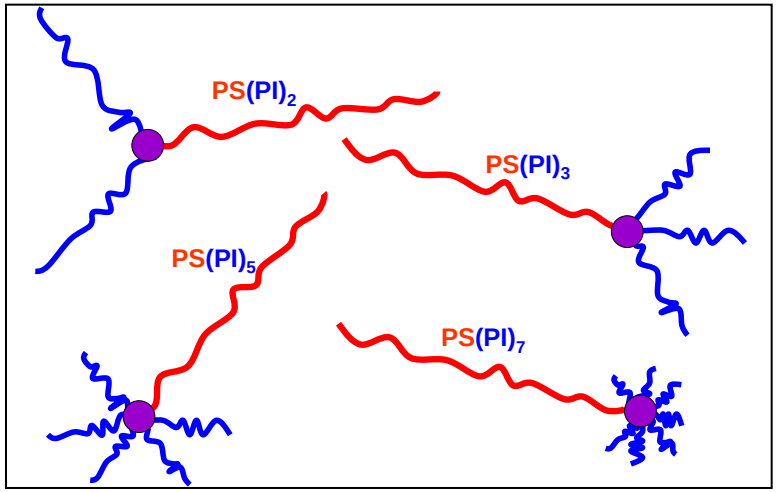

$PS(PI)_x$ Copolymer	M_n(PS) (kDa)	M_n(PI) (kDa)
$PS(PI)_2$	82	39,7
$PS(PI)_3$	82	21,0
$PS(PI)_5$	105	15,5
$PS(PI)_7$	105	11,3

Arm length

Number of arms

Macromolecules **2012**, *45*, 7574−7582

SEC/UV-MALS-RI

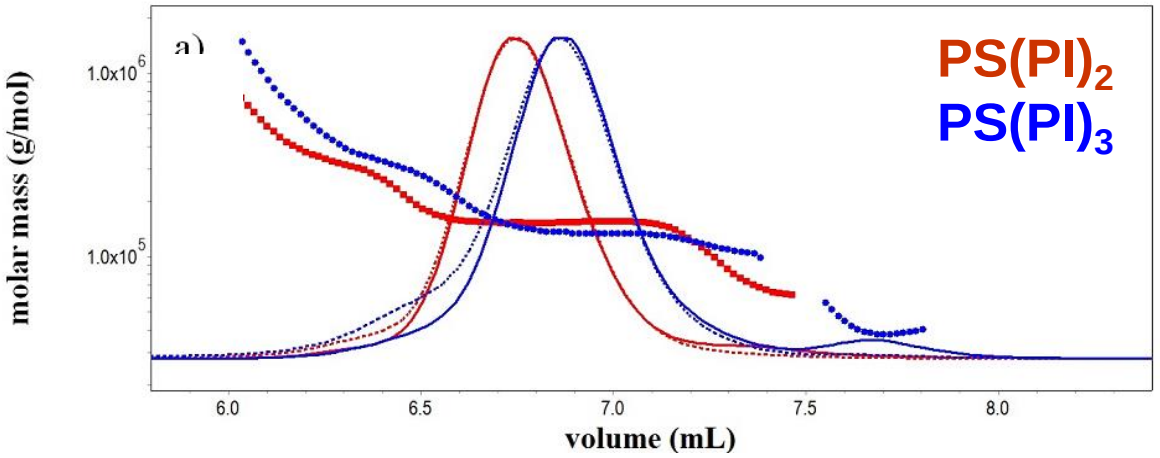

$D_M(PS(PI)_2) = 1.06$

$D_M(PS(PI)_3) = 1.14$

$D_M(PS(PI)_5) = 1.15$

$D_M(PS(PI)_7) = 1.10$

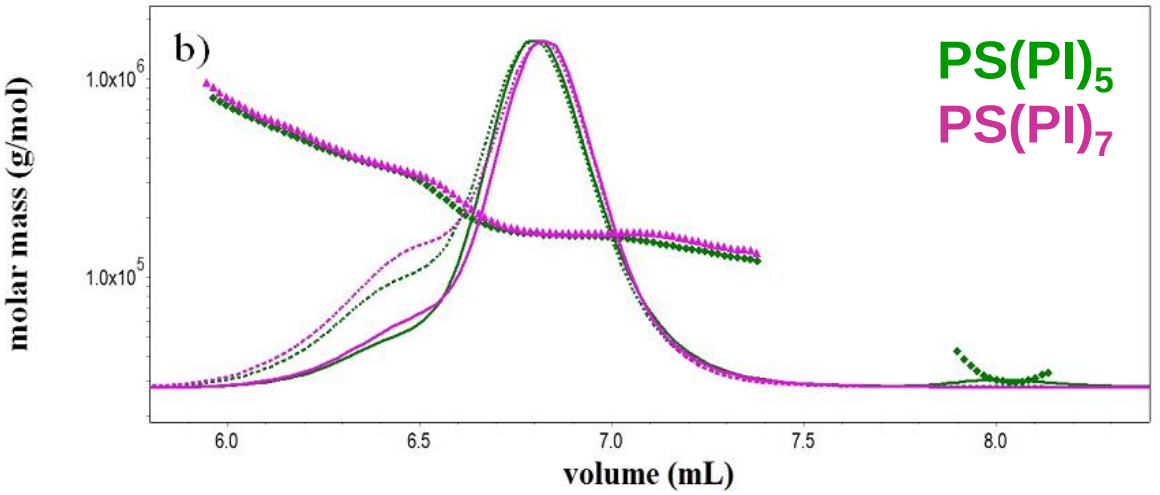

SEC/UV-MALS(QUELS)-RI

- Absolute M_n, M_w
- Dispersity, $Đ_M = M_w/M_n$
- Radius of gyration: R_g
- Hydrodynamic radius: R_h
- Conformation: R_g/R_h or $\log(R_g)$ vs. $\log(M)$
- Chemical composition if response factors of UV and RI detectors are sufficiently different.

—————— - - - - - - - - - - - .....

RI response LS response (90°) $M = f(V)$

RP-LAC Chromatograms

PI homopolymers

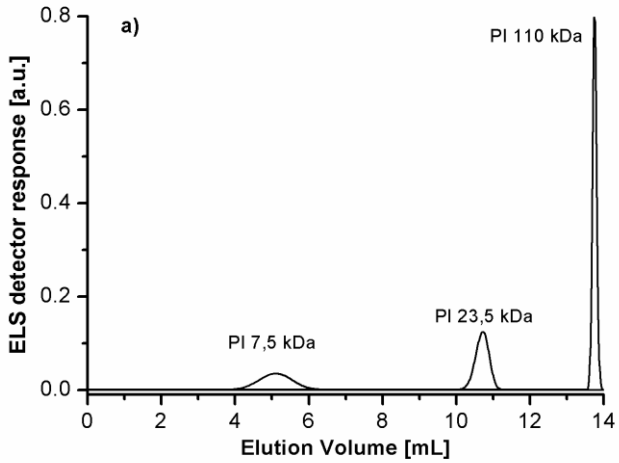

PS homopolymers

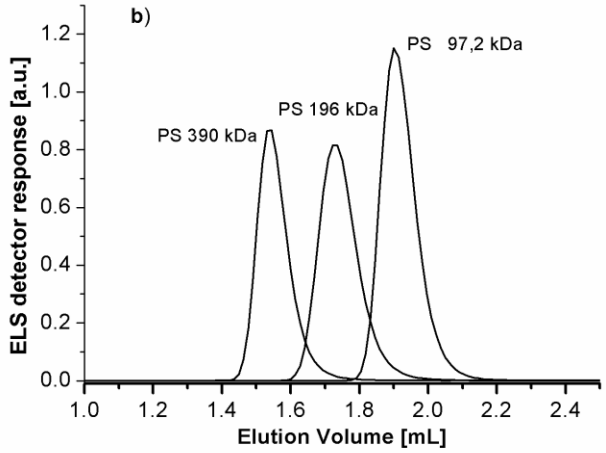

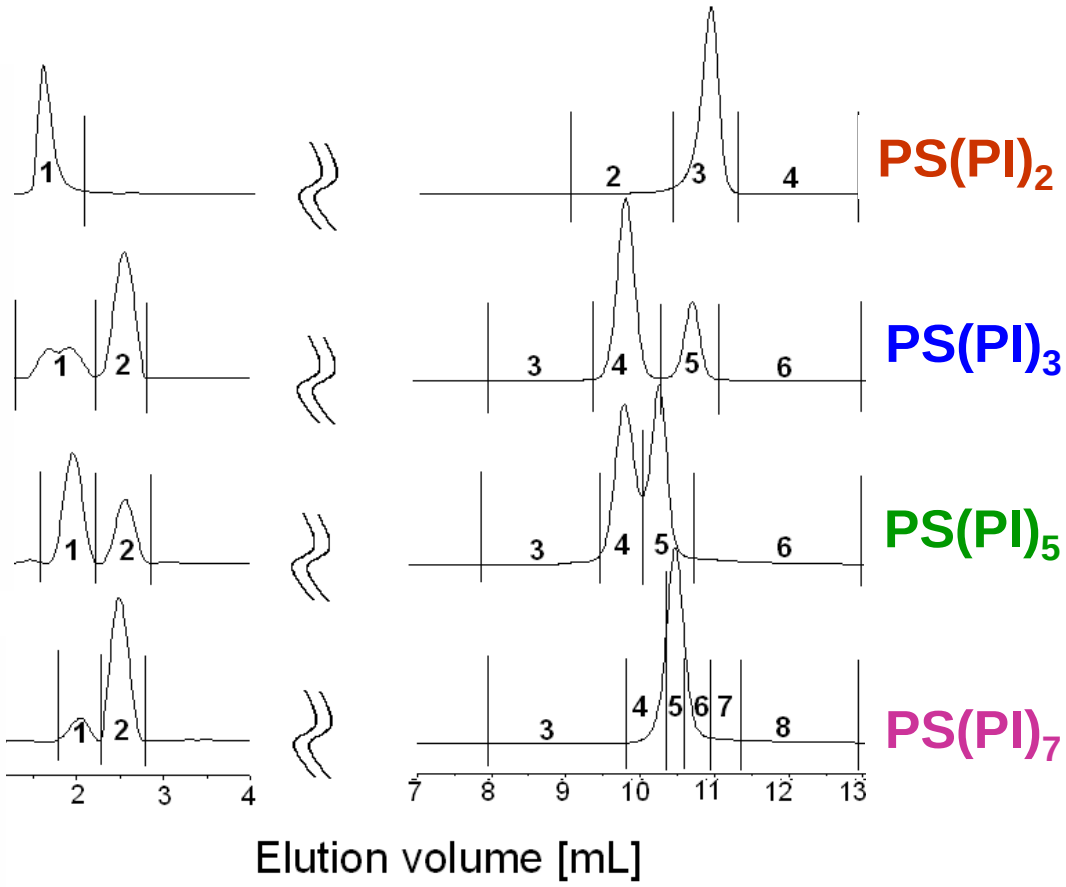

Stationary phase: C18 bonded silica column, Mobile phase: THF/ACN gradient, ELS-detector. The region between 0-4 mL is magnified.

Two-Dimensional RP-LAC × SEC Chromatography

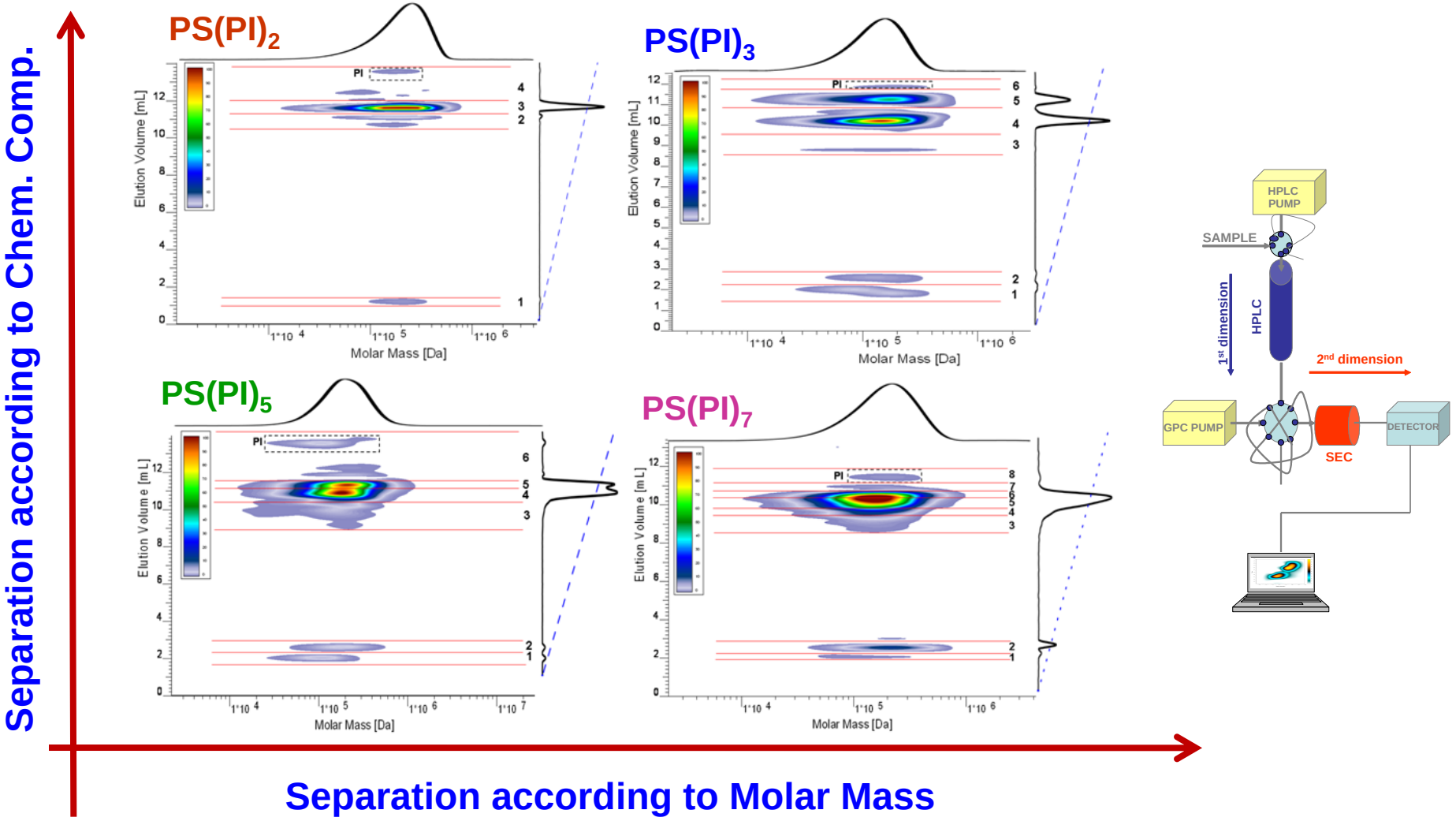

1st-D RP-LAC: a C18 bonded silica column, THF/ACN gradient.

2nd-D SEC: an SDV linear-M high-speed column, THF eluent. ELS-detector.

SEC/UV-MALS-RI of $PS(PI)_2$ and $PS(PI)_3$

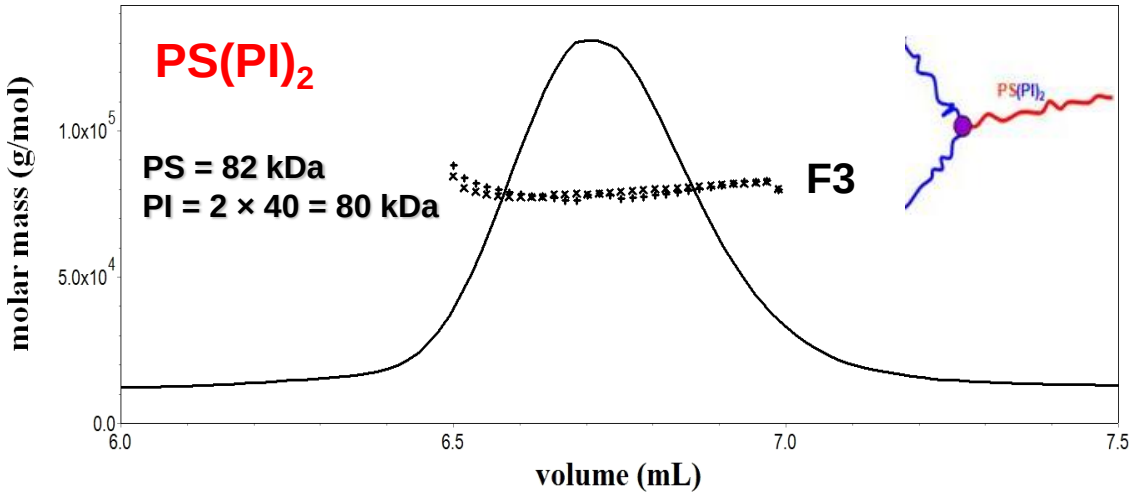

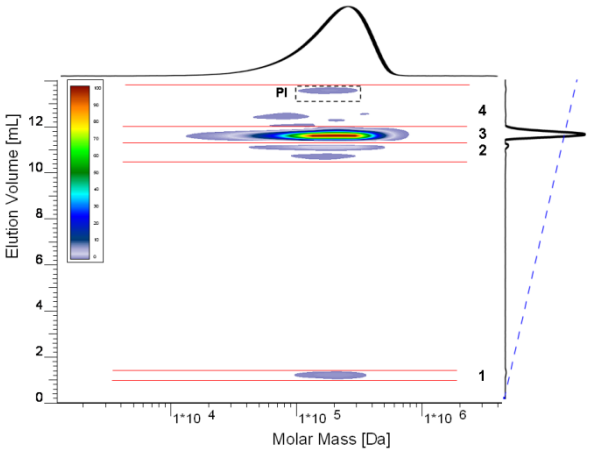

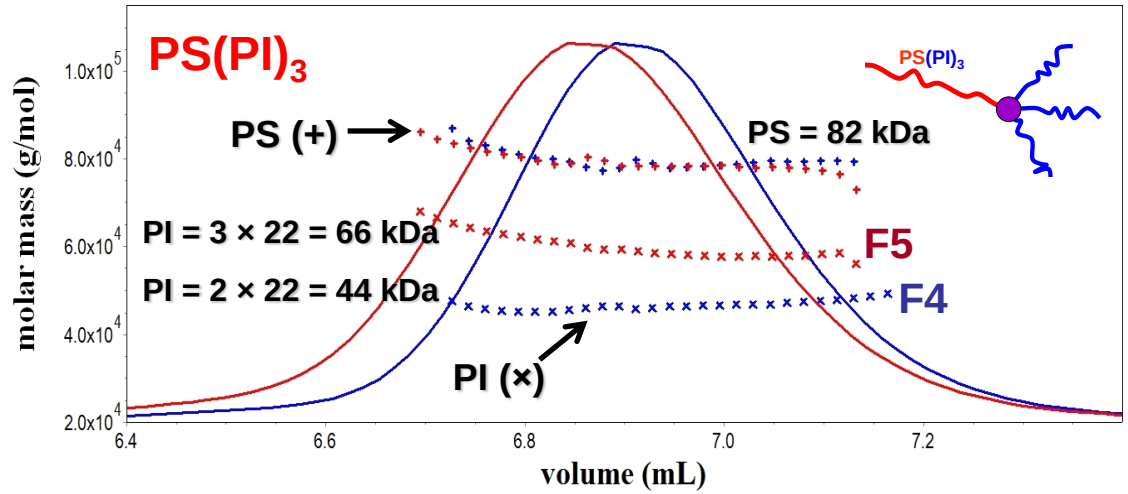

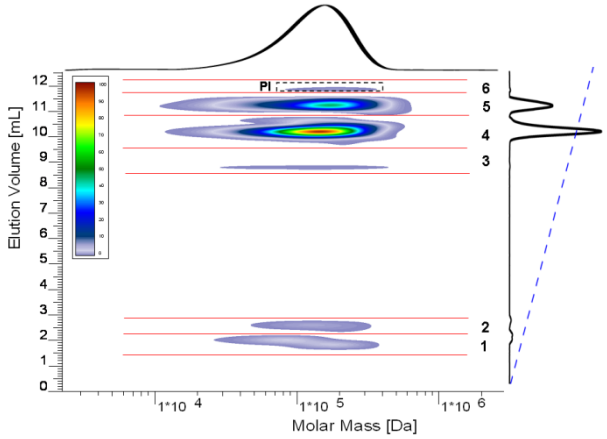

RI chromatograms of fractions and molar mass of PS and PI components vs. elution volume.

Macromolecules, 2012, 45, 7574−7582

SEC/UV-MALS-RI of $PS(PI)_5$ and $PS(PI)_6$

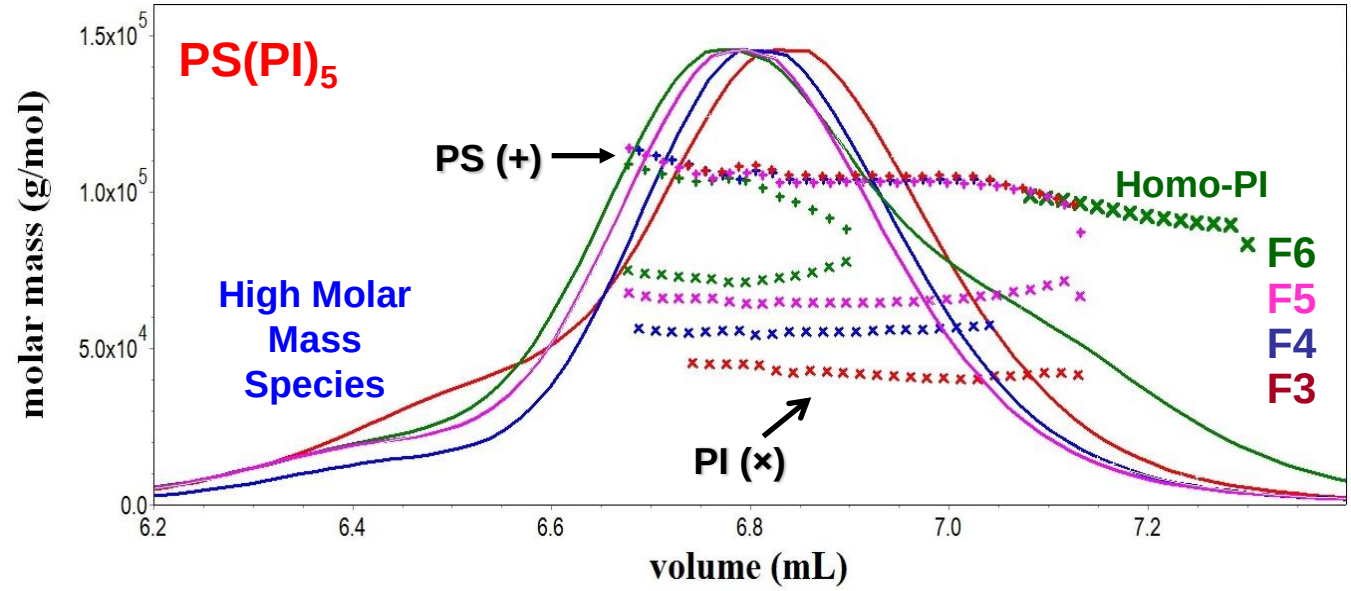

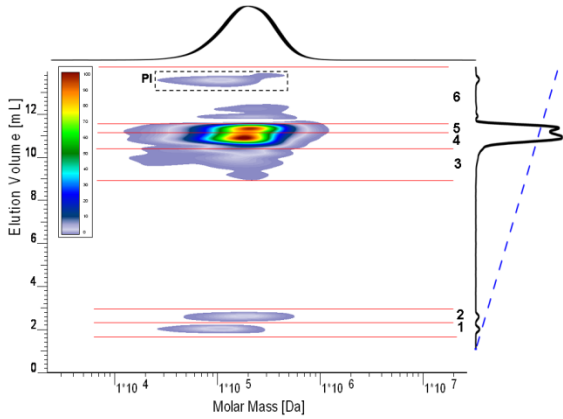

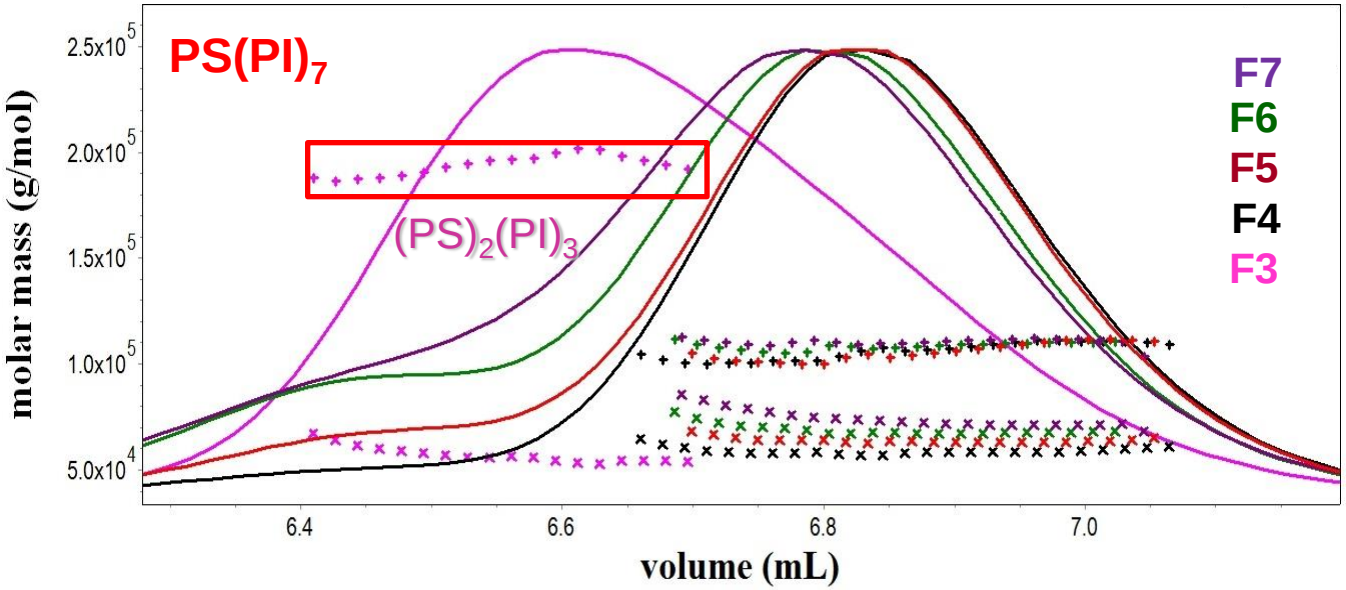

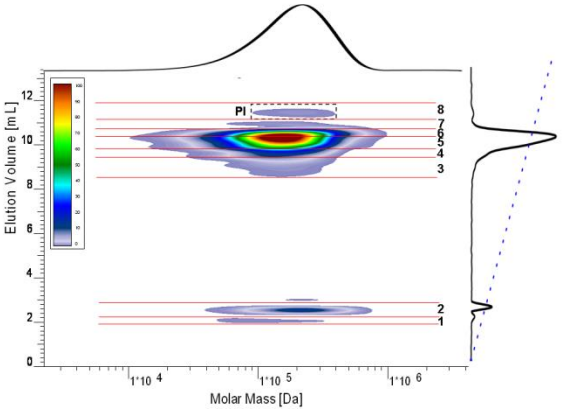

RI chromatograms of fractions and molar mass of PS and PI components vs. elution volume.

Results of characterization of fractions of $PS(PI)_x$ miktoarm star copolymers by SEC/UV-MALS-RI. The most abundant fractions in samples are red colored.

Fraction	$PS(PI)_2$	$PS(PI)_3$	$PS(PI)_5$	$PS(PI)_7$
F1	$(PS)_2$	PS + $(PS)_2$	PS	PS
F2	PSPI $(PS)_2(PI)_2$*	**	**	**
F3	$PS(PI)_2$	PSPI $(PS)_2(PI)_2$*	$PS(PI)_2$ $(PS)_2(PI)_3$*	$(PS)_2(PI)_5$ $PS(PI)_4$*
F4	$PS(PI)_2$ + $PS(PI)_3$ + PI	$PS(PI)_2$ $(PS)_2(PI)_3$*	$PS(PI)_3$ $(PS)_2(PI)_4$*	$PS(PI)_5$ $(PS)_3(PI)_{11}$*
F5		$PS(PI)_3$ $(PS)_2(PI)_4$*	$PS(PI)_4$ $((PS)_2(PI)_7$ + $(PS)_3(PI)_8 + PI_2)$*	$PS(PI)_{5.6}$ $(PS)_2(PI)_{12}$*
F6		PI_4	$PS(PI)_5$ $((PS)_2(PI)_8 + PI_6)$*	$PS(PI)_6$ $(PS)_2(PI)_{12}$*
F7				$PS(PI)_7$ $(PS)_2(PI)_{12}$*
F8				PI_7

** Fraction F2 is the breakthrough peak.

* The component represents small portion in fraction.

PEGylated granulocyte colony stimulating factor PEG-GCSF Conjugate

- **Unreacted protein, PEG**
- **Species with different degree of PEGylation**
- **Aggregates**

Two separation techniques (AF4 and SEC), both coupled to UV-MALS(QELS)-RI multidetection system.
MALDI-TOF MS.

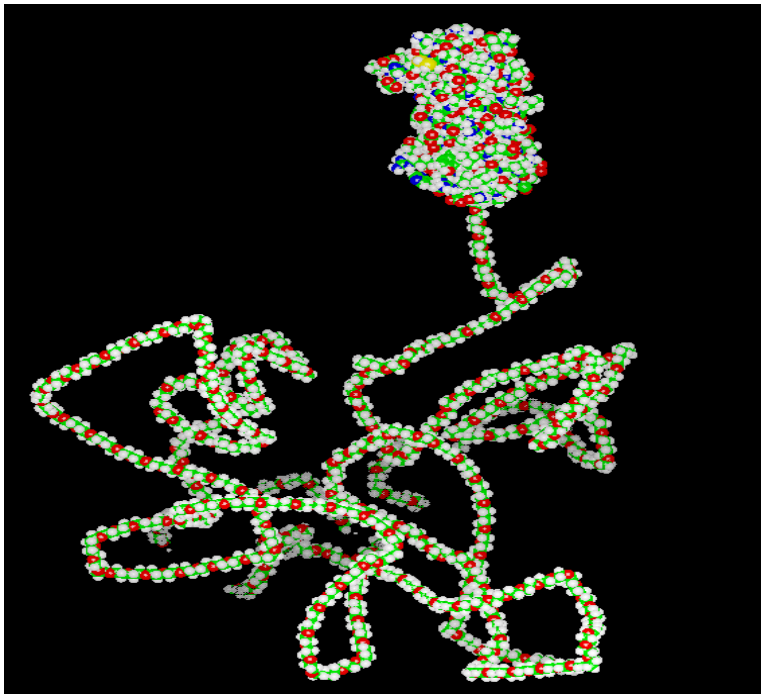

The PEGylated conjugate was stored in two buffer solutions:

- **Buffer solution 1:** 10-mM acetate buffer solution with **5% sorbitol** at pH 3.4.
  Conjugate concentration: 16.8 mg/mL.
- **Buffer solution 2:** 50-mM acetate buffer solution with 200-mM NaCl at pH 4.5.
  Conjugate concentration: 3.4 mg/mL.

Anal. Chem. **2012**, *84*, 7374−7383

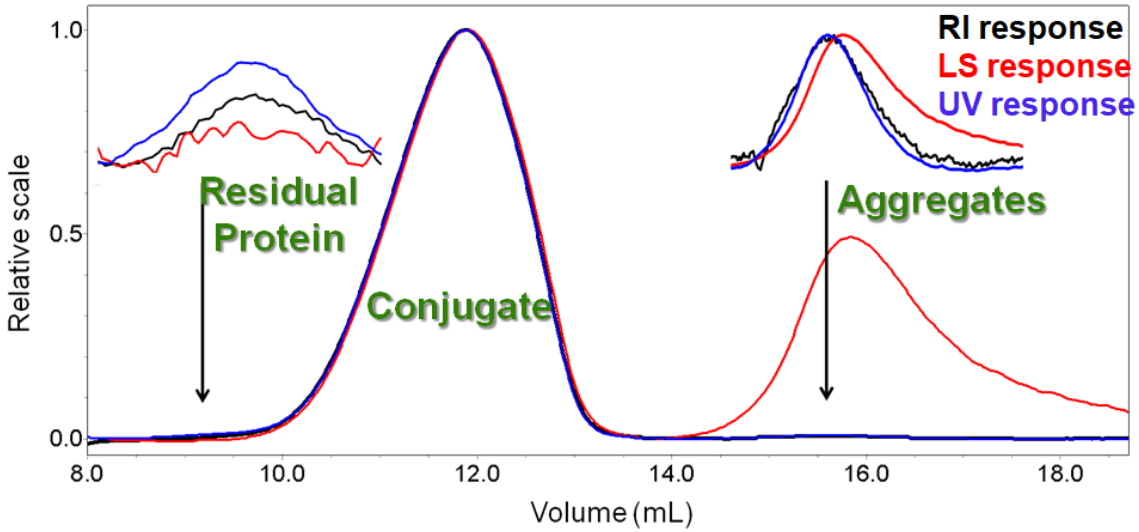

AF4 fractogram of the conjugate with enlarged regions.

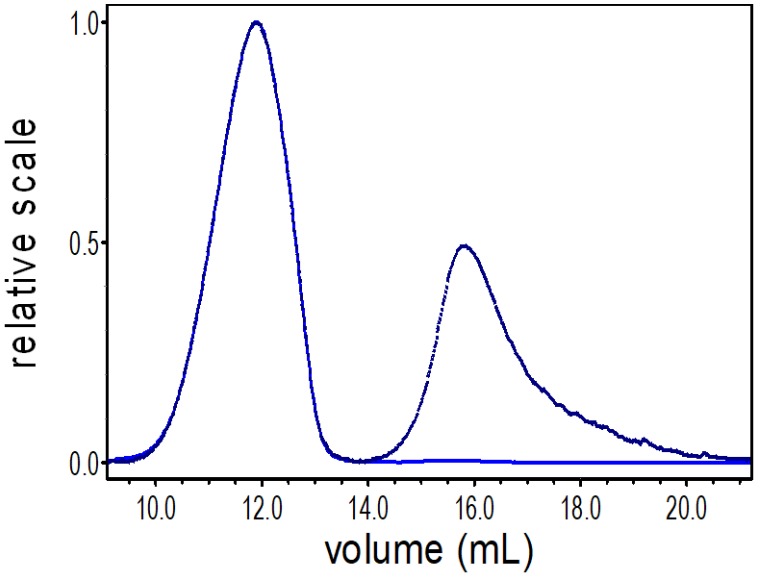

Conjugate in buffer solution 2: 5-mM acetate buffer solution, 200-mM NaCl at pH 4.5. Conjugate conc.: **3.4 mg/mL**.

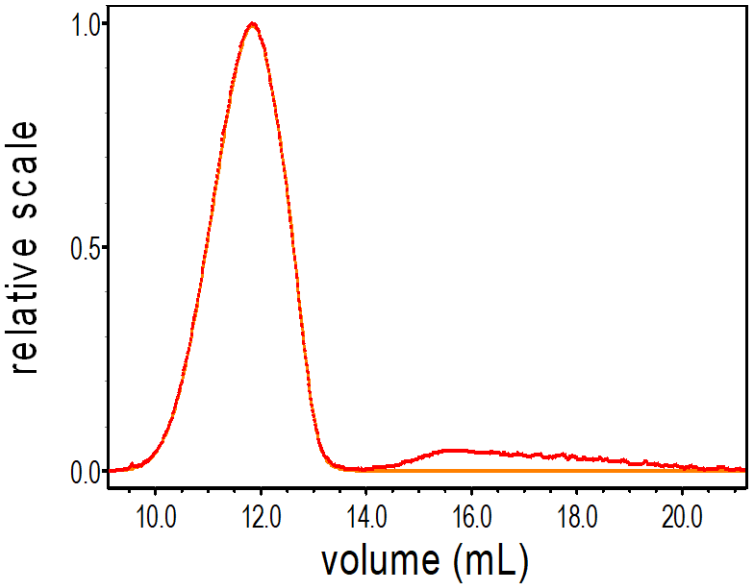

Conjugate in buffer solution 1: 10-mM acetate buffer solution, **5 % sorbitol** at pH 3.4. Conjugate conc.: **16.8 mg/mL**.

AF4/UV-MALS-RI

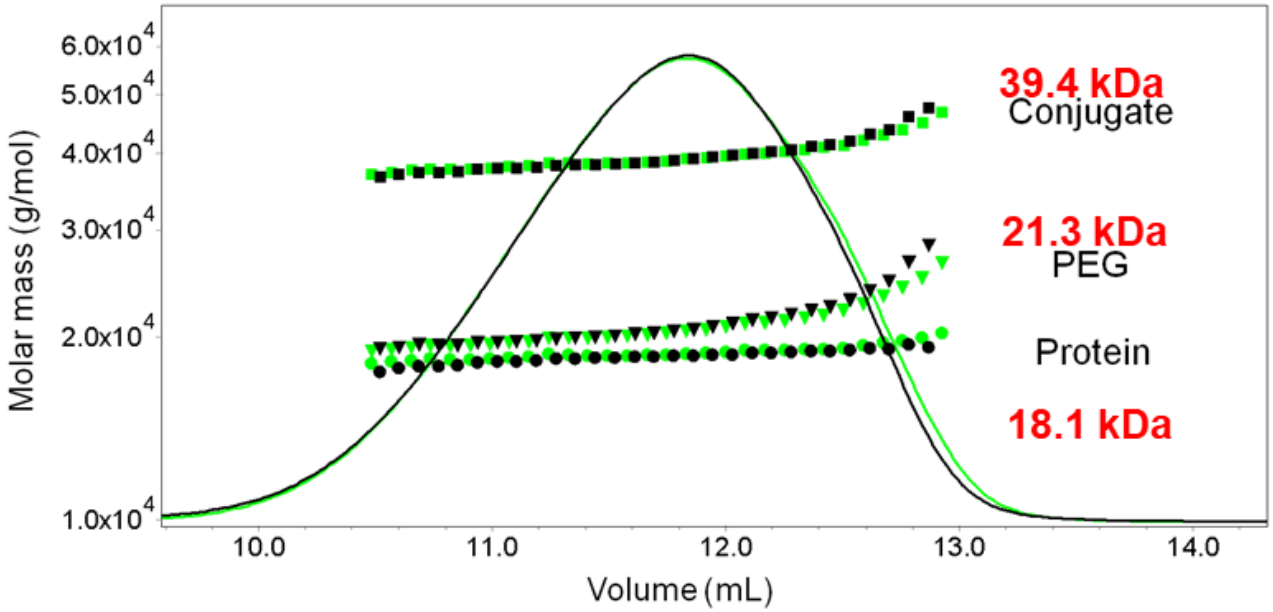

Enlarged RI fractograms of the PEGylated protein conjugate in buffer solution 1 and in buffer solution 2.

MALDI-TOF MS

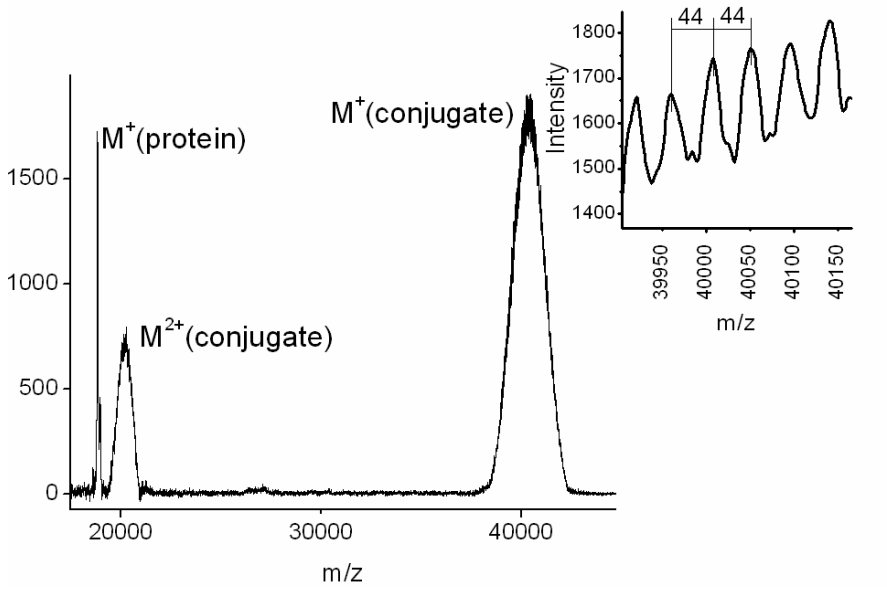

MALDI-TOF mass spectrum of the conjugate. Inset shows enlarged conjugate signal at peak appex.

Acknowledgments

- Ministry of Higher Education, Science and Technology of the Republic of Slovenia
- Slovenian Research Agency
- Department of Polymer Chemistry and Technology, NIC
- Prof. Nikos Hadjichristidis, KAUST Catalysis Center,
  King Abdullah University of Science and Technology (KAUST)
- National Institute of Biology
- Department of Biology, Biotechnical Faculty, University of Ljubljana
- Faculty of Medicine at the University of Ljubljana

Thank you for your attention!